COMPDYN 2015
5th ECCOMAS Thematic Conference on
Computational Methods in Structural Dynamics and Earthquake Engineering
M. Papadrakakis, V. Papadopoulos, V. Plevris (eds.)
Crete Island, Greece, 25–27 May 2015

PARAMETRIC EVALUATION OF VISCOUS DAMPER RETROFIT FOR HIGH-SPEED RAILWAY BRIDGES

Sarah Rådeström[1], Viktor Tell[1,2], Mahir Ülker-Kaustell[1,2] and Raid Karoumi[1]

[1]Division of Structural Engineering and Bridges, KTH Royal Institute of Technology
Brinellvägen 23, 100 44 Stockholm, Sweden
e-mail: sarah.radestrom@byv.kth.se

[2]Department of Bridges, Tyréns AB
Peter Myndes Backe 16, 118 86 Stockholm, Sweden

Keywords: Structural Dynamics, Railway Bridges, High-speed Trains, Passive Damping, Viscous Dampers.

Abstract. *Several of the bridges belonging to the Bothnia Line, located in northern Sweden, do not theoretically fulfil the current design limit for the vertical deck acceleration, when being subjected to high-speed trains. Hence, it is important to find appropriate vibration mitigation strategies that are applicable to railway bridges, in order to reduce the acceleration caused by passing trains. One way of solving this problem is to install external viscous dampers.*

A finite element solution for damper retrofit of high-speed railway bridges is proposed in this paper. The bridge is modelled as a two-dimensional Euler-Bernoulli beam, with inclined dashpots connected between the superstructure and the abutments. Furthermore, this paper highlights the influence of several parameters on the effectiveness of the dampers.

1 INTRODUCTION

The Bothnia Line is a subsection of the Swedish railway system, which stretches along the northern coastline and includes a total of 140 bridges [1]. The tracks and bridges of the line are designed for train speeds of up to 250 km/h. The maximum vertical bridge deck acceleration must not exceed 3.5 m/s^2, for bridges with ballasted tracks, according to the Eurocode [2]. However, theoretical results from previous studies [3] indicate that many of the steel-concrete composite bridges along the Bothnia Line fail to fulfil this requirement.

The demands for analyses of the dynamic behavior of high-speed railway bridges are constantly increasing, due to the combination of higher train speeds and loads together with the decreasing weight of modern railway bridges [4]. One fundamental problem that must be included in the analyses is the risk of resonance in the bridge, caused by train loading. Resonance arises when the forcing frequency from the train coincides with the eigenfrequency of the bridge, which may occur due to the periodic and repetitive action of axle loads.

Consequently, procedures for mitigating the dynamic response of structures have to be employed for both new and existing high-speed railway bridges. An efficient approach is to install control devices, in order to reduce the response of bridges subjected to passing trains [5]. Thus, the structural safety and serviceability of the bridge will be significantly increased.

One example of a damping device, which is a widely accepted application within civil structures, is the tuned mass damper (TMD). The TMD consists of a spring, an added mass and a damper and can relatively easy be attached to structures, in order to efficiently mitigate the vibrations [6]. However, the TMD is tuned to a certain frequency of the structure and will, thus, be inefficient at other ranges of frequencies [7]. Hence, inaccurate estimates of the properties of the bridge can lead to a detuning effect [8]. This results in increased installation and calibration costs, in order to tune the dampers correctly and avoid estimation errors. Furthermore, the TMD may be unsuitable for existing structures, since the structure may not be able to carry the added mass.

The fluid viscous dampers (FVD), on the other hand, provides the robustness necessary for applications in railway bridges. This type of control system covers a wide frequency band, which eliminates the detuning effect. Therefore, the installation and maintenance costs are significantly decreased. Another advantage is that the device does not consist of an added mass and will, thus, not affect the resistance of the bridge to the same extent as a TMD. Figure 1 shows a sketch of a FVD.

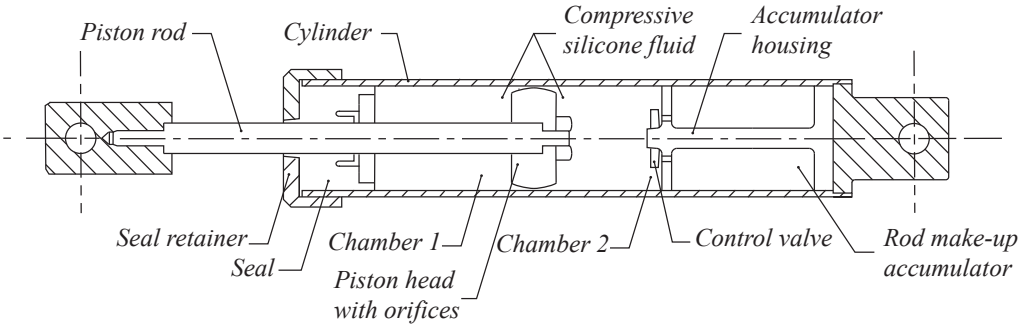

Figure 1: A sketch of a type of FVD, reproduced from [9].

Several studies include investigations of FVDs using auxiliary beams, in order to connect the dampers to the superstructure [7, 10–13]. This retrofit method (as well as installation of TMDs) may, however, be unsuitable for some bridges, where ground conditions or barriers in

the surroundings limit the accessibility for heavy construction machinery. It is expensive to restrict the traffic during the installation of the dampers, wherefore measures that have a small impact on the rail services are desirable.

This study contains a proposal of a retrofit approach, where the FVDs are installed between the superstructure and the abutments. Furthermore, the installation method imposes a distance between the neutral axis of the beam and the connection point of the damper, referred to as eccentricity in the present study. Conclusively, an investigation of some influential parameters on the efficiency of the damping properties is conducted as well.

2 NUMERICAL CALCULATIONS

The bridge is idealized as a two-dimensional Euler-Bernoulli beam, while the FVDs are modeled as dashpots and the eccentricity is obtained through constraint equations. Furthermore, the equation of motion for the system can be described by the viscously damped, linear oscillator

$$M\ddot{u} + C\dot{u} + Ku = F \tag{1}$$

where $\ddot{u}$, $\dot{u}$ and u are the acceleration, velocity and displacement of the structural components. Moreover, M, C and K are the matrices of the mass, damping and stiffness, respectively, and F is the force. The damping consists of the damping contribution from the external dampers C_{d} and the structural damping of the bridge C_{s}. Hence, the governing equation of motion for the bridge-damper system can be expressed as

$$M\ddot{u} + [C_{\mathrm{d}} + C_{\mathrm{s}}]\dot{u} + Ku = F \tag{2}$$

The calculation of the train forces is based on a procedure that is described by Frỳba [14]. The axle distances and loads determine the magnitude and position of the forces at each time instant. These values correspond to the high-speed load model (HSLM) trains that are stated in the Eurocode [2].

The force matrix is assembled by assuming a linear interpolation between the nodes, in order to find the distribution of each concentrated force to the closest vertical degree-of-freedom (DOF) at each time step. The nodal forces at each time instant are shown in Equation (3), where the indices i and $i+1$ correspond to the vertical DOF that the force has already passed and the one it will pass in the immediate future, respectively.

$$F_i(t) = \sum_{n-1}^{N} F_n \epsilon_n(t) \left[\frac{ct - d_n - d_i}{d_{i+1} - d_i} \right] \tag{3a}$$

$$F_{i+1}(t) = \sum_{n-1}^{N} F_n \epsilon_n(t) \left[1 - \frac{ct - d_n - d_i}{d_{i+1} - d_i} \right] \tag{3b}$$

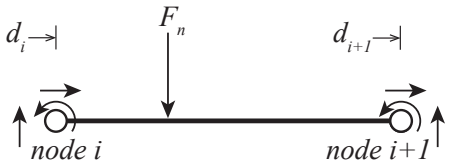

Figure 2: A sketch of the moving concentrated force acting on a beam element.

The quantities in Figure 2 and Equation (3) are the axle force of the nth train axle F_n, the train speed c, the time t and the distance between the first force and the nth force d_n. d_i and d_{i+1} are the positions of the two nodes of the loaded element, whereas $i = 1, 2, 3, ..., N_y - 1$ and N_y is the number of vertical DOFs along the beam. Furthermore, ϵ_n is a function that determines whether or not the force is acting on the beam and is defined as

$$\epsilon_n(t) = H\left[t - t_n\right] - H\left[t - T_n\right] \tag{4}$$

where t_n and T_n are the times when the nth force enters and exits the bridge (with a total bridge length L), respectively

$$\begin{aligned} t_n &= d_n/c \\ T_n &= [L + d_n]/c \end{aligned} \tag{5}$$

and $H(t)$ is Heaviside's function, given by

$$H(t) = \begin{cases} 0 & \text{for } t < 0 \\ 1 & \text{for } t \geq 0 \end{cases}$$

Thereafter, direct time integration using the implicit Newmark's method is conducted, in order to obtain the maximum bridge deck acceleration and velocity at each time instant. The first step is to initialize the values for the force, $F_0 = 0$, and displacement $u_0 = 0$, as well as its derivatives, $\dot{u}_0 = 0$ and $\ddot{u}_0$

$$\ddot{u}_0 = \frac{F_0 - C\dot{u}_0 - Ku_0}{M} \tag{6}$$

The same applies for the Newmark's coefficients, a_1, a_2 and a_3. These depend on the mass and the damping of the system.

$$\begin{aligned} a_1 &= \frac{\beta\Delta t^2}{M} + \frac{\gamma}{\beta\Delta t}C \\ a_2 &= \frac{\beta\Delta t}{M} + \frac{\gamma - \beta}{\beta}C \\ a_3 &= \frac{1 - 2\beta}{2\beta}M + \frac{\gamma - 2\beta}{2\beta}C\Delta t \end{aligned} \tag{7}$$

The constants β and γ in Equation (7) are the Newmark's average acceleration parameters, which are 0.25 and 0.5 respectively. After the initialization, the following procedure is then performed for each time step, Δt.

$$\begin{aligned} \hat{K} &= K + a_1 \\ \hat{F} &= F_{t+1} + a_1 u_t + a_2 \dot{u}_t + a_3 \ddot{u}_t \end{aligned} \tag{8}$$

which gives the displacement, velocity and acceleration at time $t + 1$

$$\begin{aligned} u_{t+1} &= \hat{F}/\hat{K} \\ \dot{u}_{t+1} &= \frac{\gamma}{\beta\Delta t}\Delta u_t + \frac{\beta - \gamma}{\beta}\dot{u}_t + \frac{2\beta - \gamma}{2\beta}\ddot{u}_t\Delta t \\ \ddot{u}_{t+1} &= \frac{1}{\beta\Delta t^2}\Delta u_t - \frac{1}{\beta\Delta t}\dot{u}_t - \frac{1 - 2\beta}{2\beta}\ddot{u}_t \end{aligned} \tag{9}$$

where $\Delta u_t = u_{t+1} - u_t$. Equations (8) and (9) are then repeated for all time steps.

The values for $\dot{u}$ and $\ddot{u}$ in Equation (9) are then used to derive the maximum acceleration and calculate the damper force. The maximum acceleration is found by collecting the maximum value of $\ddot{u}$, at any time instant, for each train speed. Furthermore, the maximum velocity in the dampers must be determined, in order to calculate the required damper force according to Equation (10).

$$f_{\mathrm{d,max}} = c_{\mathrm{d}} |\dot{u}_{\mathrm{max}}| \tag{10}$$

The constant c_{d} in Equation (10) is the damping coefficient for the external damper. The maximum velocity, $\dot{u}_{\mathrm{max}}$, is obtained by extracting the maximum velocity at the damper connections, for all time steps and each train speed.

3 CASE STUDY

A case study of one of the bridges along the Bothnia Line, which theoretically fails to fulfil the Eurocode acceleration requirement, is performed. The investigated bridge (see Figure 3) is called the Banafjäl Bridge. It is a simply supported, single track, steel-concrete composite girder bridge. The relevant bridge properties are shown in Table 1, where the given quantities are: Young's modulus E, the eccentricity e (i.e. the distance between the neutral axis of the bridge and the connection point of the damper, see also Figure 4), the area moment of inertia I, the span length L, the mass of the bridge m and the damping ratio of the constituent materials ξ (chosen according to recommendations in [2]).

Figure 3: The Banafjäl Bridge.

Table 1: Properties of the Banafjäl Bridge.

E	*e*	*I*	*L*	*m*	ξ
[GPa]	[m]	[m^4]	[m]	[kg/m]	[%]
200	2.2	0.61	42	18 400	0.5

Figure 4 shows the proposed retrofit, where c_{d} is the damping coefficient for the external dampers, e is the eccentricity between the bridge deck neutral axis and the connection point of

the dampers (which is assumed to coincide with the vertical coordinate of the support point). Furthermore, α is the inclination of the dampers and x_{d} is the distance between the support and the connection point of the dampers. On this bridge, dampers could be installed using cross beams, attached between the bottom flanges of the main girders.

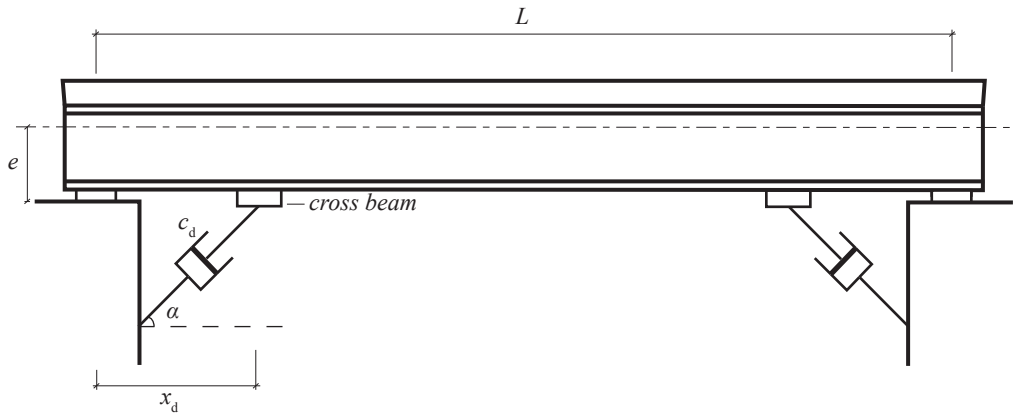

Figure 4: The proposed retrofit method of the dampers.

Previous studies [3] have shown that the critical HSLM-train for this bridge is the HSLM-A4 (see [2]), so the following investigations are limited to this train. The speed of the train, during the passages of the bridge, is varied from 100-300 km/h, with a speed increment of 1 km/h.

4 PARAMETRIC EVALUATION

Four different parameters are varied within the scope of this study, in order to observe the impact on the damping properties, namely;

- the damping coefficient of the dampers
- the eccentricity between the neutral axis of the bridge and the damper connections
- the inclination of the dampers
- the distance from the supports to the connection points of the dampers

Only one of the different parameters are changed within each investigation, while the remaining variables are held constant. The damping coefficient is changed to $c_{\mathrm{d}} = 0, 2, 3, 4.5$ MNs/m. Moreover, the eccentricity is altered between the following values: $e = 0, 2.2, 2.6, 3.0$ m. The first two values, $e = 0$ m and $e = 2.2$ m, correspond to the cases when the dampers are attached directly to the neutral axis of the bridge and to the lower flanges of the girders, respectively. The remaining values are the eccentricity together with two different heights of the additional cross beam (i.e. 0.4 m and 0.8 m). The inclination of the dampers is varied between $\alpha = 30, 45, 60, 75°$ and the distance from the support to the connection point of the dampers is increased within an interval of $x_{\mathrm{d}} = 1, 2, 3, 4$ m. A prerequisite for the evaluations of α and x_{d} is that elongation of the dampers is possible, without introducing any impairments of the stiffness or damping properties. The results in the following sections are presented in the form of maximum acceleration and required damper force as a function of train speed. From Figure 5, it is clear that the bridge has a resonance condition at a speed about 168 km/h.

4.1 The damping coefficient

Figure 5 shows the result of varying the damping coefficient while keeping the eccentricity, inclination and distance from the support constant as $e = 2.2$ m, $\alpha = 45°$ and $x_{\mathrm{d}} = 1$ m, respectively. The top figure shows the acceleration levels for different values of the damping coefficient and train speeds. The bottom figure shows the corresponding damper forces.

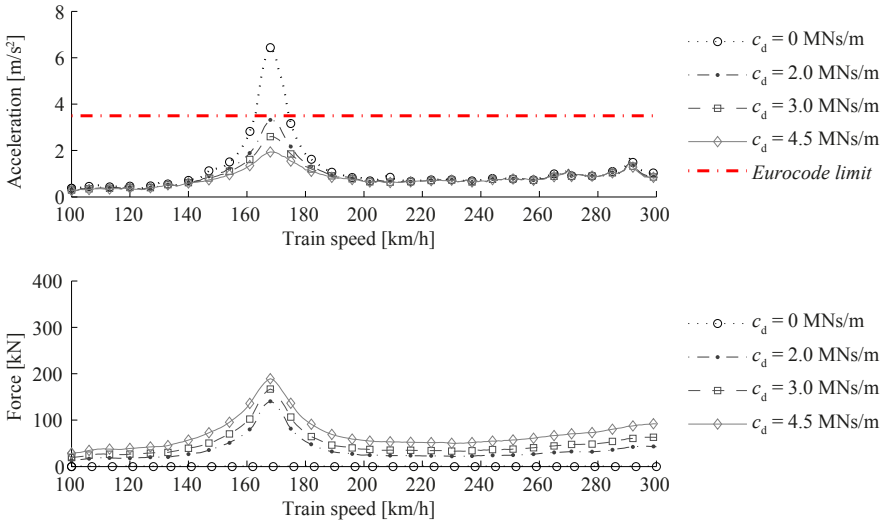

Figure 5: The maximum acceleration and damper force at different train speeds and damping coefficients.

4.2 The eccentricity

Figure 6 includes the results when the height of the cross beam (and, hence, eccentricity) is altered. The upper figure gives the amplitude of the acceleration after the damper retrofit with varying eccentricities and a constant damping coefficient $c_{\mathrm{d}} = 4.5$ MNs/m. Both the damper inclination and the distance from the support is fixed as $\alpha = 45°$ and $x_{\mathrm{d}} = 1$ m, respectively. Moreover, the lower figure shows the required damper force, when altering the same parameter.

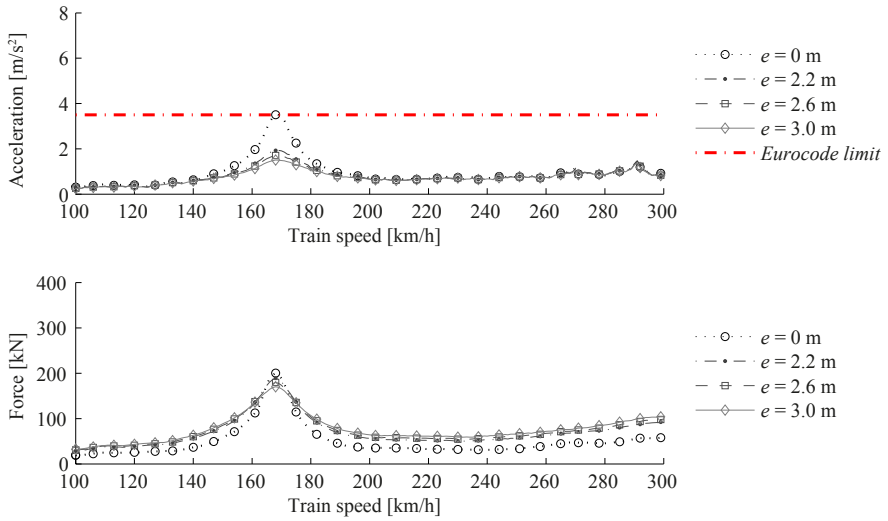

Figure 6: The maximum acceleration and damper force at different train speeds and eccentricities.

4.3 The damper inclination

The results in Figure 7 show the impact on the damping properties when changing the inclination of the damper, with a constant damping coefficient $c_\mathrm{d} = 4.5$ MNs/m, eccentricity $e = 2.2$ m and distance from support $x_\mathrm{d} = 1$ m. The upper and lower figures show the acceleration and force for different inclinations and train speeds, respectively.

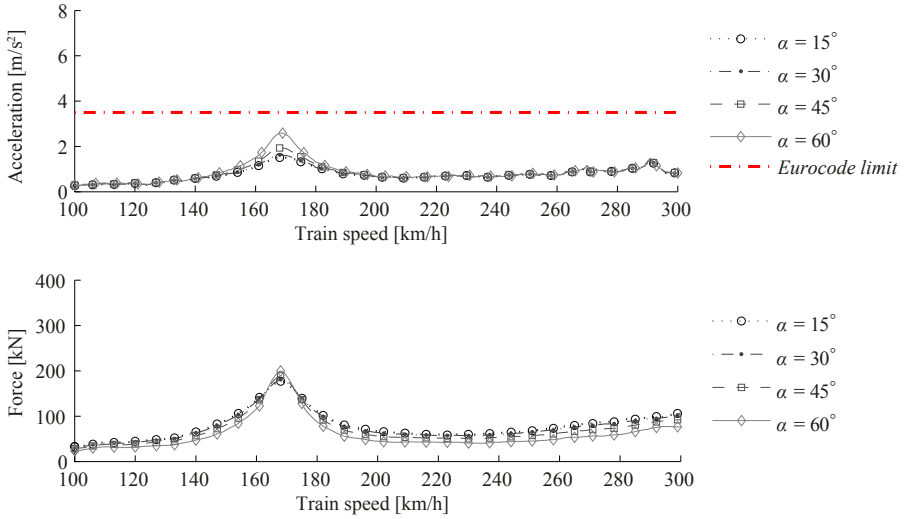

Figure 7: The maximum acceleration and damper force at different train speeds and damper inclinations.

4.4 The distance from the supports

Figure 8 shows the influence of the distance from the supports to the damper connections, while the damping coefficient is $c_\mathrm{d} = 4.5$ MNs/m, the eccentricity is $e = 2.2$ m and the damper inclination is $\alpha = 45°$. The figure shows the impact on the maximum acceleration and the damper force.

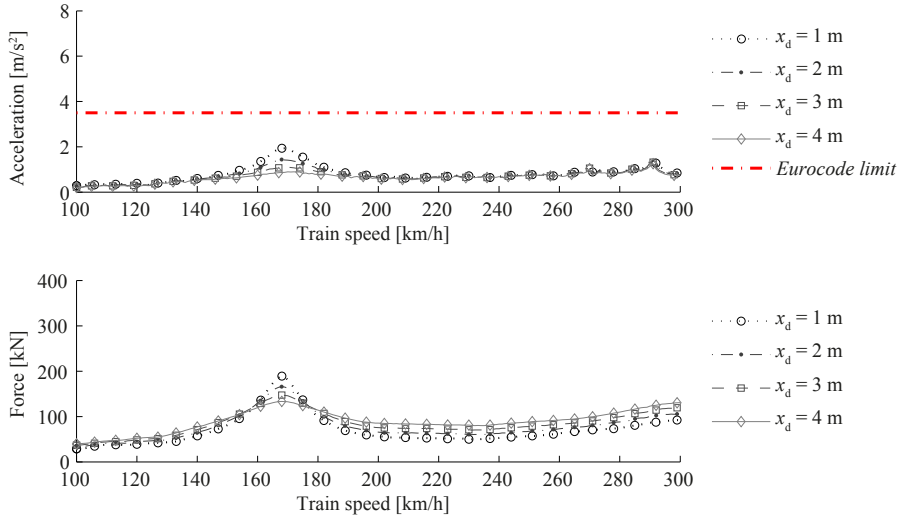

Figure 8: The maximum acceleration and damper force at different train speeds and distances from support.

5 DISCUSSION

The results from Figure 5 to Figure 8 indicate that the bridge deck vertical accelerations can be significantly reduced, when using FVDs according to the proposed attachment method. As expected, the dampers are most efficient for the reduction of the vibrations at resonance, which arises at the critical train speed. The acceleration level only exceeds the design code limit at resonance for this particular bridge, therefore the dampers are efficient for this case.

As shown in Figure 5, the damping coefficient has a major impact on the results. Theoretically, the acceleration can be reduced from 6.4 m/s^2 to 3.3 m/s^2 and 1.9 m/s^2, when using damper coefficients of 2.0 MNs/m and 4.5 MNs/m, respectively. However, the required damper force increases with the damping coefficient. This is important to consider when using FVDs as a retrofit approach for existing bridges.

The height of the cross beam affects the acceleration level, which is shown in Figure 6. Both the acceleration and damper force are lower for a longer distance between the neutral axis and the connection point of the dampers. Thus, an optimal eccentricity exists for each individual bridge, which must be considered in the design of the cross beam.

The dampers are more effective when installed with an angle between 15°-30° to the horizontal plane, than for steeper inclinations (see Figure 7). A reason for this is that the eccentricity of the bridge gives a rotational contribution to the movement of the connection point of the dampers. This results in a more prominent horizontal movement. A less steep angle is, thus, preferred, since the damper device is only able to operate in its axial direction.

From Figure 8, it is clear that the acceleration and the damper force at resonance are further reduced, as the distance to the midpoint of the bridge decreases. Hence, the optimal connection point of the dampers is further out from the support. However, the effect seems to diminish, as the distance between the support and the connection point of the dampers increases. Furthermore, the possible positions of the attachment point are limited, since a connection point further from the support requires a longer damper. This may lead to a lower stiffness of the device and, thereby, a reduced damping capacity.

The proposed solution can be optimized and adapted to many different bridge configurations. However, this retrofit method may lead to problems that have to be investigated and remedied. As seen in the results presented here, the effectiveness of the FVDs is sensitive to changes of certain parameters. Hence, it is important that all uncertainties of the bridge-damper system are accurately and appropriately accounted for in the analysis.

ACKNOWLEDGEMENTS

Deep gratitude is directed to the Department of Bridges at Tyréns AB for helping out in the beginning of the study and, thereby, making this research possible.

REFERENCES

[1] J Wiberg and R Karoumi. *Kontroll av dynamiska effekter av passerande tåg på Botniabanans broar: Sammanfattning*. KTH Department of Structural Engineering and Bridges, 2006. (In Swedish).

[2] European Committee for Standardization (CEN). Eurocode 1: Actions on structures - part 2: Traffic loads on bridges. EN 1991-2, 2003.

[3] C Johansson, A Andersson, C Pacoste, and R Karoumi. *Järnvägsbroar på Botniabanan: Dynamiska kontroller för framtida höghastighetståg – Steg 1*. KTH Department of Structural Engineering and Bridges, 2013. (In Swedish).

[4] JW Kwark, ES Choi, YJ Kim, BS Kim, and SI Kim. Dynamic behavior of two-span continuous concrete bridges under moving high-speed train. *Computers & Structures*, 82(4):463–474, 2004.

[5] HC Kwon, MC Kim, and IW Lee. Vibration control of bridges under moving loads. *Computers & Structures*, 66(4):473–480, 1998.

[6] GL Lin, CC Lin, BC Chen, and TT Soong. Vibration control performance of tuned mass dampers with resettable variable stiffness. *Engineering Structures*, 83:187–197, 2015.

[7] MD Martínez-Rodrigo, J Lavado, and P Museros. Dynamic performance of existing high-speed railway bridges under resonant conditions retrofitted with fluid viscous dampers. *Engineering Structures*, 32(3):808–828, 2010.

[8] JF Wang, CC Lin, and BL Chen. Vibration suppression for high-speed railway bridges using tuned mass dampers. *International Journal of Solids and Structures*, 40(2):465–491, 2003.

[9] DP Taylor and MC Constantinou. *Fluid dampers for applications of seismic energy dissipation and seismic isolation*. Taylor Devices, Incorporated, 1998.

[10] P Museros and MD Martínez-Rodrigo. Vibration control of simply supported beams under moving loads using fluid viscous dampers. *Journal of Sound and Vibration*, 300(1):292–315, 2007.

[11] MD Martínez-Rodrigo and P Museros. Optimal design of passive viscous dampers for controlling the resonant response of orthotropic plates under high-speed moving loads. *Journal of Sound and Vibration*, 330(7):1328–1351, 2011.

[12] J Lavado, A Doménech, and MD Martínez-Rodrigo. Dynamic performance of existing high-speed railway bridges under resonant conditions following a retrofit with fluid viscous dampers supported on clamped auxiliary beams. *Engineering Structures*, 59:355–374, 2014.

[13] M Luu, MD Martínez-Rodrigo, V Zabel, and C Könke. H_∞ optimization of fluid viscous dampers for reducing vibrations of high-speed railway bridges. *Journal of Sound and Vibration*, 333(9):2421–2442, 2014.

[14] L Frỳba. A rough assessment of railway bridges for high speed trains. *Engineering Structures*, 23(5):548–556, 2001.